

Combined Self-Assembled iRGD Polymersomes for Effective Targeted siRNA Anti-Tumor Therapy

Dongying Li^{1,2,*}, Jiarun Li^{1,2,*}, Siwei Wang^{1,2}, Wei Teng², Qinmei Wang¹

¹Laboratory of Biomaterials, Key Laboratory on Assisted Circulation, Ministry of Health, Cardiovascular Division, First Affiliated Hospital, Sun Yat-sen University, Guangzhou, People's Republic of China; ²Hospital of Stomatology, Guangdong Provincial Key Laboratory of Stomatology, Institute of Stomatological Research, Guanghua School of Stomatology, Sun Yat-sen University, Guangzhou, People's Republic of China

*These authors contributed equally to this work

Correspondence: Wei Teng; Qinmei Wang, Email tengwei@mail.sysu.edu.cn; wangqinm@mail.sysu.edu.cn

Introduction: iRGD is usually used as a motif to modify siRNA-nanodelivery vectors to improve tumor-targeting and penetration. However, most of the modifications are realized by covalent conjugation, which normally requires complex preparation processes possibly with low conjugation efficiency and yield, and might lower its bioactivity. To avoid this, here, we presented an alternative physical method to decorate iRGD on nanopolymersomes via facile self-assembly in water.

Methods: *siVEGF* was chosen as a siRNA model, and lipopolysaccharide-amine nanopolymersomes (NPs), an efficient cytosolic delivery vector developed by our group, was used as an original vector. By successively incubating *siVEGF* with NPs, followed by adding iRGD, a *siVEGF*-loaded NPs functionalized with iRGD (siRNA/iRGD-NPs) was obtained. The properties of iRGD-NPs or siRNA/iRGD-NPs were evaluated in vitro and in vivo.

Results: iRGD is efficiently introduced onto NPs with different amounts, which can be precisely controlled by the feeding ratio. The introduced iRGD keeps tumor-targeting and -penetrating bioactivity, which endows iRGD-NPs with ~100% of tumor-cell uptake and excellent tumor spheroid-penetration, and thus iRGD-NPs can efficiently deliver *siVEGF* to significantly inhibit angiogenesis in zebrafish and tumor growth in nude mice bearing breast cancer without obvious toxicity.

Conclusion: This study provides a facile physical method to decorate nanodelivery vectors with iRGD for effective targeted siRNA anti-tumor therapy.

Keywords: iRGD-decorated nano-delivery system, self-assembly, tumor targeting & penetrating, nanopolymersomes, small interfering RNA, anti-tumor therapy

Introduction

Small interfering RNA (siRNA) is considered a revolutionary tool for tumor therapy via specifically silencing genes related to tumor progression.¹⁻⁵ However, the lack of safe and efficient tumor-targeting and penetrating delivery vectors has limited the clinical applications of siRNAs, because siRNAs are unstable under harsh in vivo milieu and they have no ability to enter target tissues and cells without the help of delivery vectors. To solve these problems, a lot of functional nanoparticle vectors have been designed through tumor-targeting ligand modification strategies, which can deliver siRNA to tumors via active targeting (from ligands) and passive targeting (from nanoparticles due to the enhanced permeability and retention (EPR) effect of tumors). To date, a number of tumor-targeting ligands such as proteins, peptides and vitamins have been identified and exploited.⁴⁻⁷ Among them, the tumor-penetrating internalized RGD (iRGD, CRGDK/RGPD/EC) peptide has attracted much attention because of its excellent tumor targeting and penetration capability.^{4,5,7,8}

iRGD is a cyclic peptide containing a tumor/neovascular-specific RGD motif, a CendR tissue penetration motif (CRGDR/K), and a protease recognition site.^{4,5,7-10} Theoretically, for iRGD-modified nanocarriers in the systemic delivery, the RGD motif first specifically recognizes and binds to $\alpha_v\beta$ integrins, which are highly expressed on tumor

neovascular endothelial cells and tumor cells, but lowly or barely expressed on mature vascular endothelial cells and normal cells, and thus, the targeted delivery of iRGD-modified nanocarriers to tumors, including tumor cells and tumor neovascularization endothelial cells, was promoted. Next, iRGD is in-situ proteolytically cleaved into CRGDR/K and GPD/EC fragments. The CRGDR/K binds to NRP-1, which induces iRGD-modified nanocarriers out of the tumor vessels and deep into extravascular tumor tissues via the endocytosis and transecytosis. As a result, tumor tissue targeting accumulation and deep penetration of iRGD-modified nano-delivery systems are realized. Due to the large number of tumor cells and neovascular endothelial cells in the tumor, iRGD modification of nanocarrier is especially effective in tumor targeting and penetration for anti-tumor therapy, and much progress has been made in this field. For example, Guan et al developed an iRGD-functionalized liposome to deliver antisense oligonucleotides (ASOs), and found that this delivery system can significantly increase ASO accumulation and efficacy in solid tumors without significant side effects, thus increasing the antitumor efficacy of ASOs.¹⁰ Wang et al prepared iRGD-modified graphene oxide (GO) nanosheets (IPHG), and demonstrated that iRGD modification endowed IPHG with tumor-selective infiltration, and transendothelial and intratumoral transport.¹¹ Yin et al synthesized a type of cylindrical polymer brushes with side chains terminated by iRGD, and studied the effects of iRGD conjugation density on their tumor-targeting and -penetrating ability. They discovered that the higher the conjugation density, the larger the cellular uptake, tumor accumulation, and tumor spheroids penetration depth.¹²

Although iRGD-modification can increase the tumor-targeting and -penetrating ability of nanodelivery systems, most of the modifications are realized by covalent conjugation, which normally requires a complex preparation process possibly with limited conjugation efficiency and yield.^{8,10-12} Additionally, such complicated preparation is costly, time-consuming, and unfriendly to the environment and clinical translation, and may affect the activity of iRGD. To address this issue, this study was to develop an alternative physical method to introduce iRGD into nanodelivery systems via electrostatic and hydrophilic/hydrophobic interactions. Lipopolysaccharide-amine copolymer (LPSA), developed by our group,¹³ was chosen as a raw material for target vector construction due to the following reasons. Firstly, LPSA has a structure suitable for the physical bonding of iRGD. LPSA consists of hydrophobic cholesteryl and hydrophilic cationic polyethyleneimine (PEI 1.8k) and anionic oxidized alginate (OA), where OA and cholesteryl-graft-PEI act as backbones and side chains, respectively (Figure S1). Such amphoteric and amphiphilic structure gives LPSA the ability to spontaneously self-assemble into nanopolymersomes in water via electrostatic and hydrophobic interactions, either by itself or with anionic nucleic acids such as pDNA and siRNA. The formed LPSA nanopolymersomes (NPs) has a PEI corona and a hydrophobic membrane composed of cholesteryl and polyelectrolyte complexes of PEI and OA.¹³⁻¹⁶ Since iRGD is a peptide with amphotericity and amphiphilicity, we conjecture that NPs might have the ability to physically bind iRGD by electrostatic and hydrophobic/hydrophilic interactions, which might be easily realized by coincubation of NPs and iRGD in water (Figure S1B). Secondly, NPs is an efficient cytosolic delivery vector, which can efficiently deliver pDNA and siRNA in vitro and in vivo: when delivering *pEGFP*, >95% transfection efficiency in mesenchymal stem cells (MSCs) can be reached;¹³ when delivering *pVEGF*, significant and dose-dependent angiogenesis in zebrafish can be induced without obvious toxicity;¹⁶ when delivering *siNoggin*, 50% of Noggin expression can be silenced, and thus the osteogenic differentiation of MC3T3 E1 cells is significantly enhanced.¹⁴ Based on these, we guessed that after being decorated by iRGD, NPs would have an enhanced ability in tumor-targeted delivery of siRNA, and thus leading to increased anti-tumor efficacy.

To test our hypothesis on decorating nanodelivery vectors with iRGD via a facile physical method to improve their tumor-targeting and -penetrating ability, in this study, we prepared iRGD-functionalized Lipopolysaccharide-amine nanopolymersomes (iRGD-NPs) and *siVEGF*-loaded Lipopolysaccharide-amine nanopolymersomes functionalized with iRGD (*siVEGF*/iRGD-NPs) via a successive coincubation method, and then evaluated their tumor-targeting and -penetrating activity, and the efficacy in anti-angiogenesis and tumor-growth inhibition by in vitro and in vivo experiments. It is worth noting that, because angiogenesis is a key process in the growth, survival, invasiveness, and metastasis of tumors, and anti-angiogenesis has been proved an efficient anti-tumor therapy, here, we chose VEGF siRNA (*siVEGF*) as a model siRNA.⁴

Materials and Methods

Lipopolysaccharide-amine polymer (LPSA) was synthesized according to our reported method, and the nitrogen content and mass ratios of OA:PEI:Cho were controlled to be 11.29 mmol/g and 48.5:11.2:40.3, which has been demonstrated to have optimal cytosolic delivery and low cytotoxicity.^{13–16} 1 mg/mL of LPSA nanopolymersomes (NPs) was prepared by directly dissolving LPSA in nuclease-free sterile water with mild stirring at room temperature, and kept at 4°C as a stock solution for subsequent experiments. iRGD was bought from GL Biochem Corporation Ltd. (Shanghai, China). Micro-BCA assay kit was purchased from ThermoFisher SCIENTIFIC (Guangzhou, China). Cy5-siRNA (non-coding nonfunctional siRNA labeled by Cy5 fluorophore) and VEGF small interfering RNA (*siVEGF*) were purchased from RiBoBio (Guangzhou, China), whose sequence information was presented in [Table S1](#), and used according to the provider's protocol. Mesenchymal stem cells (MSCs) from SD rats were purchased from Cyagen Biosciences Inc. (Guangzhou, China). MCF-7 cell line was obtained from National Collection of Cell Cultures. Transgenic *flk1:EGFP* zebrafish containing fluorescently labeled endothelial cells were kindly provided by Centre for Translational Medicine, Sun Yat-sen University, China. Female nude mice (4 weeks old, 15–18 g) were purchased from the Laboratory Animal Center of Sun Yat-sen University (Guangzhou, China). All animal care and experimental procedures were performed according to Institutional Animal Care and Use Guidelines and approved by the “Animal Ethics Committee” of Sun Yat-sen University. The other reagents were purchased from local suppliers. Unless otherwise stated, all reagents were used as received without further purification, a weight ratio was used for all recipes of siRNA/iRGD-NPs preparation, and 50 nM siRNA and 0.5 mg/kg siRNA per intravenous injection was used for in vitro cell experiments and in vivo tests, respectively.

The Preparation and Characterization of iRGD-Functionalized Lipopolysaccharide-Amine Nanopolymersomes

For preparation of iRGD-functionalized lipopolysaccharide-amine nanopolymersomes (iRGD-NPs), NPs solution (1 mg/mL) was vortex mixed with an equal volume of iRGD solution with different concentrations, followed by incubation at room temperature for different time. Then, these solutions were transferred into an ultrafiltration tube (MWCO:50 kDa), and centrifuged at 7500g for 15 minutes to remove free iRGD. The amount of free iRGD in filtrates was determined by micro-BCA kit according to the supplier's instructions. The iRGD binding to NPs was calculated as follows: $\text{Mass}_{\text{bound iRGD}} = \text{Mass}_{\text{initial iRGD}} - \text{Mass}_{\text{removed free iRGD}}$, the encapsulation efficiency (EE) = $\text{Mass}_{\text{bound iRGD}} / \text{Mass}_{\text{initial iRGD}} \times 100\%$, and the loading efficiency (LE) = $\text{Mass}_{\text{bound iRGD}} / (\text{Mass}_{\text{bound iRGD}} + \text{Mass}_{\text{NPs}}) \times 100\%$. The effects of incubation time and weight feeding ratio on iRGD loading by NPs were investigated. It should be noted that the centrifugal ultrafiltration can thoroughly separate free iRGD from iRGD-NPs, which was verified by micro-BCA kit: the absorbance of filtrate from the second centrifugation at 562 nm is zero. We defined iRGD-decorated NPs as iRGD-NPs-n, where n is the weight ratio of NPs to iRGD (NPs/iRGD). The morphology of particles was observed with a JEM-200 transmission electron microscope (TEM, JEOL, Japan) using a negative staining technique,^{13,16} and their size and zeta potential were analyzed by a Zetasizer (Nano-ZS90, Malvern, Britain) using the functions of dynamic light scattering (DLS) and zeta-potential.

The Cytotoxicity Studies of iRGD Functionalized Lipopolysaccharide-Amine Nanopolymersomes to Mesenchymal Stem Cells

Cytocompatibility, especially to normal somatic cells, is a prerequisite for in vivo siRNA delivery systems. We evaluated the cytotoxicity of iRGD-NPs to rMSCs using AlamarBlue (Invitrogen) (n = 6) according to the supplier's protocol. Briefly, rMSCs (1×10^4 cells/well) were seeded in 96-well plates and routinely cultured overnight in complete medium, then exposed to a culture medium containing 35 $\mu\text{g/mL}$ NPs or iRGD-NPs with different concentrations of bound iRGD for 4 hours' incubation, followed by 44 hours' routine culture in complete medium. Thereafter, cells were treated by AlamarBlue for cell viability assay. The cell viability was expressed as the percentage of the absorbance of sample-treated cells relative to that of untreated cells. It has to be pointed out that, 35 $\mu\text{g/mL}$ NPs was chosen for cytotoxicity

experiments because according to our previous experiments, it is the optimal concentration for pDNA transfection,^{13,16} which is much higher than that (3.35 $\mu\text{g/mL}$) for optimal siRNA transfection.¹⁴

The Stability of iRGD-Functionalized Lipopolysaccharide-Amine Nanopolymerosomes in Different Environments

The stability of iRGD-NPs against different environments was investigated by monitoring the changes in size and zeta potential of nanopolymerosomes determined by DLS. We first explored the storage stability of lyophilized iRGD-NPs at 4 °C for one year. Then, their stability in various simulant physiological environments, including against dilution (350 ~ 17.5 $\mu\text{g/mL}$) and serum (20% serum in PBS) was studied.¹⁵

The Preparation and Characterization of siRNA-Loaded Lipopolysaccharide-Amine Nanopolymerosomes

siRNA-loaded NPs (siRNA/NPs) was prepared following our established method (Figure S1).¹⁴ Briefly, NPs solution with different concentrations was vortex mixed with an equal volume of siRNA solution, followed by incubation at room temperature for different time. Then, some of these solutions were immediately used for agarose gel electrophoresis to assay the binding ability of NPs to siRNA (gel retardation assay) and the effect of incubation time on binding; some were used for ultrafiltration (MWCO:50 kDa) at 7500g for 15 minutes to collect free siRNA, whose concentration in filtrates was determined by micro-BCA kit for calculating encapsulation efficiency. These studies show that, siRNA can be complexed by NPs in 15 minutes at NPs/siRNA ≥ 1.25 g/g with 100% encapsulation efficiency (Figure S2), and thus the weight ratio of NPs/siRNA > 1.25 and coincubation time of 15 minutes were used for preparing siRNA/NPs.

The Preparation and Characterization of siVEGF-Loaded Lipopolysaccharide-Amine Nanopolymerosomes Functionalized with iRGD

The preparation of siRNA-loaded NPs functionalized with iRGD (siRNA/iRGD-NPs) includes two steps. First, siRNA was co-incubated with NPs in water to prepare siRNA/NPs complexes; second, siRNA/NPs was co-incubated with iRGD in water to obtain siRNA/iRGD-NPs complexes (Figure S1). It should be noted that, our preliminary experiment results show that siRNA/iRGD-NPs at NPs/siRNA/iRGD = 9/1/1 (weight ratio) can achieve excellent transfection effect in vitro and in vivo, and thus this weight ratio was chosen for constructing all systems in this paper, unless otherwise stated. In a typical procedure, 1 mL of 239.4 $\mu\text{g/mL}$ NPs was mixed thoroughly and incubated with 1 mL of 26.6 $\mu\text{g/mL}$ siRNA for 15 minutes,¹⁴ and then 2 mL of 26.6 $\mu\text{g/mL}$ iRGD was added and continuously incubated for 240 minutes to obtain siRNA/iRGD-NPs complexes with a weight feeding ratio of NPs/iRGD/siRNA = 9/1/1.

In our preliminary experiments, to test whether siRNA and iRGD were completely complexed by NPs, and free siRNA and iRGD did not exist in solutions in step 1 and step 2 under the above preparation conditions, we performed tests same as those in the parts of preparation and characterization of siRNA/NPs (iRGD-NPs). The analysis of agarose gel electrophoresis showed that no free siRNA existed in solutions of step 1 and step 2, and micro-BCA assay confirmed that no free iRGD existed in the solution of step 2 (data not shown), suggesting the successful construction of siRNA/iRGD-NPs. Then the morphology and size of siRNA/iRGD-NPs were measured by TEM and DLS. The as-prepared complex solution was used for in vitro cell experiments.

Screening of Target Cells Highly Expressing $\alpha_v\beta_3$ Integrin and NPR-1

WesternBlot analysis was performed using a standard method to screen target cells that highly express $\alpha_v\beta_3$ integrin and NPR-1. Briefly, four kinds of tumor cells (MCF-7, 293T, 293FT, and HeLa) were routinely cultured, collected, and lysed for extraction of total protein. The concentration of total protein was determined with micro-BCA assay kit following supplier's protocol. Then the proteins were separated with 8% sodium dodecyl sulfate polyacrylamide gel electrophoresis and transferred to polyvinylidene difluoride membranes. After blocking with bovine serum albumin, membranes were overnight incubated with primary antibody against NPR-1 or $\alpha_v\beta_3$ integrin or GAPDH at 4 °C. Then, the membranes

were incubated with secondary antibody for 1 h at room temperature. The blot signals were detected using ECL Plus (Millipore, Billerica, MA, USA).

Cellular Uptake Studies on siRNA-Loaded Lipopolysaccharide-Amine Nanopolymersomes with or Without iRGD Functionalization

The cellular uptake study was conducted using Cy5-labeled siRNA as a fluorescent indicator. Cy5-siRNA/iRGD-NPs and Cy5-siRNA/NPs were prepared as described above. MCF-7 cells were seeded in 24-well plates at a density of 1×10^5 cells/well in complete DMEM and cultured for 24 hours, followed by exposure to a serum-free culture medium containing 35 $\mu\text{g}/\text{mL}$ of Cy5-siRNA/iRGD-NPs or Cy5-siRNA/NPs and 50 nM siRNA. At designed time points, cells were washed with ice-cold PBS thrice. Subsequently, some cells were stained with DAPI and observed under a confocal laser-scanning microscopy (Nikon A1R, Japan), and the others were digested with trypsin, collected by centrifugation, and resuspended in PBS containing 0.5% paraformaldehyde for determining the percentage of fluorescent-positive cells and the average fluorescence intensity per cell with a coulter flow cytometer (Becton-Dickinson).

Endocytosis Pathway of siRNA-Loaded Lipopolysaccharide-Amine Nanopolymersomes Functionalized with iRGD

MCF-7 at ~70% confluency was cultured in fresh medium containing different inhibitors including iRGD (500 μM), anti-ApoER2 (1 $\mu\text{g}/\text{mL}$, Invitrogen), adamantanamine (20 μM), amiloride (2.5 mM), genistein (1 mM), and sodium azide (100 mM) in 24-well plates for 1 h, then incubated in serum-free medium containing Cy5-siRNA/iRGD-NPs-9 (35 $\mu\text{g}/\text{mL}$ of NPs) for 4 h, and the percentage of fluorescence-positive cells and the average fluorescence intensity were analyzed with a coulter flow cytometer using a routine method as described above.

Tumor Spheroid Penetration of siRNA-Loaded Lipopolysaccharide-Amine Nanopolymersomes with or Without iRGD Functionalization

Tumor spheroids of MCF-7 were prepared by hanging drop method.¹⁷ Briefly, 20 μL of cell suspension with different cell concentrations was dropped onto the lid of a culture dish (100 mm^2), then the lid was inverted over a dish containing 10 mL of serum-free medium, and the hanging drop of cells was routinely incubated for 24–96 h to form a two-dimensional aggregate. Thereafter, the cell aggregates were transferred into 96-well plates coated with agar using a Pasteur pipette, and routinely cultured in DMEM for 48–96 h to form three-dimensional spheroids. The effects of preparation conditions on MCF-7 spheroid formation, including cell concentration in hanging drops, culture time on lids and on agar were investigated.

Thereafter, the resulting tumor spheroids were cultured with Cy5-siRNA/iRGD-NPs and Cy5-siRNA/NPs for 4 h, respectively. Next, the tumor spheroids were washed thrice by ice-cold PBS, fixed in 4% formaldehyde for 30 min, and observed under a laser confocal microscope (LSM780, Zeiss, Germany). The images were analyzed by ImageJ software to determine the relative fluorescence intensity at different depths.

Toxicity and Anti-Angiogenesis Induced by siVEGF-Loaded Lipopolysaccharide-Amine Nanopolymersomes in Zebrafish

siVEGF/NPs complexes were freshly prepared for transfection by mixing 250 μL of 1 μM siVEGF and 250 μL of NPs solution with different concentrations (0.5, 0.67, and 1 mg/mL). The culture and reproduction of zebrafish followed our established method.¹⁶ Briefly, zebrafish embryos were produced by natural pairwise mating and cultured at 28.5 $^\circ\text{C}$ in Holt buffer, an aqueous solution containing 3.5 g/L NaCl, 0.05 g/L KCl, 0.025 g/L NaHCO_3 , and 0.1 g/L CaCl_2 . At 24 hours post fertilization (hpf), 20 healthy embryos were transferred into 6-well plates, and cultured in 5 mL Holt buffer containing 0.025 mM 1-phenyl-2-thiourea (PTU) and 500 μL siVEGF/NPs complexes, where the final concentration in culture medium was 50 nM for siVEGF and 25, 33.5, and 50 $\mu\text{g}/\text{mL}$ for NPs, respectively. Triplicate wells were set for each concentration, and embryos untreated were used as controls. At 72 hpf, zebrafish were taken out, and observed and imaged under an inverted Olympus DP70 epifluorescence

microscope (Olympus, Tokyo, Japan) for evaluation of survival rate and anti-angiogenesis efficacy. For the anti-angiogenesis assay, the overall length and area of sub-intestinal vessel (SIV) in zebrafish were quantified by Image-proplus software.

Toxicity and Anti-Angiogenesis Induced by *siVEGF*-Loaded Lipopolysaccharide-Amine Nanopolymersomes Functionalized with iRGD in Zebrafish

siVEGF/iRGD-NPs were freshly prepared for transfection in zebrafish with an equal volume of *siVEGF*/NP solution and iRGD solution with different concentrations including 0, 50, 100, 200, 400, and 800 $\mu\text{g/mL}$. It should be noted that 1 mg/mL of NPs and 1 μM *siVEGF* were chosen for *siVEGF*/iRGD-NPs complex preparation based on the results of transfection of *siVEGF*/NPs in zebrafish, which leads to efficient anti-angiogenesis and survival rate suitable for in vivo application. The procedure of transfection in zebrafish for *siVEGF*/iRGD-NPs is similar to that for *siVEGF*/NPs except that, at 24 hpf, zebrafish embryos in 6-well plates were treated with solution of *siVEGF*/iRGD-NPs instead of *siVEGF*/NPs. At 72 hpf, some zebrafish were taken out for determination of survival rate and area/length of SIV in zebrafish, and the others for gene-silencing efficiency by quantifying the level of expressed VEGF mRNA with quantitative real-time polymerase chain reaction (qRT-PCR) according to our previously reported method.¹⁴ In brief, zebrafish were collected for homogenate. Afterwards, the total RNA in zebrafish was extracted using Trizol reagent, reversely transcribed into cDNA, amplified, and assayed by qRT-PCR instrument (LightCycler[®]480 SYBR Green I Master, Roche). The expression level of VEGF gene was calculated by the $\Delta\Delta C_T$ method using GAPDH as an endogenous reference, and untreated group as a blank control.

Tumor Inhibition of *siVEGF*-Loaded Lipopolysaccharide-Amine Nanopolymersomes Functionalized with iRGD in Nude Mice Bearing Breast Cancer

Based on our aforementioned experiment results from cells and zebrafish, and the reported data on *siVEGF*-delivering nanomedicine for anti-tumor therapy from references,^{18–20} for safety and efficiency, we chose *siVEGF*/iRGD-NPs with weight ratio of NPs:iRGD:*siVEGF* = 9:1:1 for anti-tumor test in mice, and *siVEGF*/NPs and saline were used as controls. Female nude mice bearing breast cancer were established by subcutaneous injection of MCF-7 cells (4×10^6 cells in 0.2 mL PBS) at breast pad. Mice were routinely raised, and the volume of the tumor was monitored. When the tumor grew to 60–70 mm^3 , the nude mice were randomly divided into 3 groups (normal saline (blank control), *siVEGF*/NPs, and *siVEGF*/iRGD-NPs) ($n = 5$). Drugs were administrated by tail vein injection at a *siVEGF* dose of 0.5 mg/kg per time every three days for five times.^{19,21} Tumor volume and animal weight were measured every 3 days till 14 days post administration.^{19,20} The tumor length (L) and width (W) were measured to calculate tumor volume (V) using the following equation: $V = 1/2 \times L \times W^2$. The inhibition rate of tumor growth (%) = $(V_{\text{saline}} - V_{\text{test}}) / V_{\text{saline}} \times 100\%$, where V_{saline} and V_{test} is the tumor volume of saline group and nanomedicine group, respectively.

Mice were humanely sacrificed two days after the last administration, and the tumor tissue was harvested and weighed. Thereafter, the weighed tissue was homogenized in ice cold normal saline using a routine method, and the supernatant was separated and frozen at -80°C for future test. The concentration VEGF protein in supernatants was determined using a Rat VEGF ELISA Kit (Boster) according to the manufacturer's instructions. The VEGF protein level in breast tumor tissues were expressed as $\text{pg VEGF/mg tumor tissue}$, and the relative VEGF protein level of nanomedicine group to saline group = $\text{VEGF}_{\text{test}} / \text{VEGF}_{\text{saline}} \times 100\%$, where $\text{VEGF}_{\text{saline}}$ and $\text{VEGF}_{\text{test}}$ is the VEGF content in tumor of saline group and nanomedicine group, respectively.

Statistics Analysis

Each experiment was performed at least three times. Data were expressed as mean \pm standard deviation. A two-tailed Student's t -test was used for statistical analysis unless otherwise specified. $P < 0.05$ is considered statistically significant.

Results

Loading Capacity of Lipopolysaccharide-Amine Nanopolymersomes to iRGD

We introduced iRGD into LPSA nanopolymersomes (NPs) by a simple self-assembly method. The loading capacity of NPs to iRGD was investigated. Figure 1A presents the effects of incubation time on iRGD loading at a weight feeding

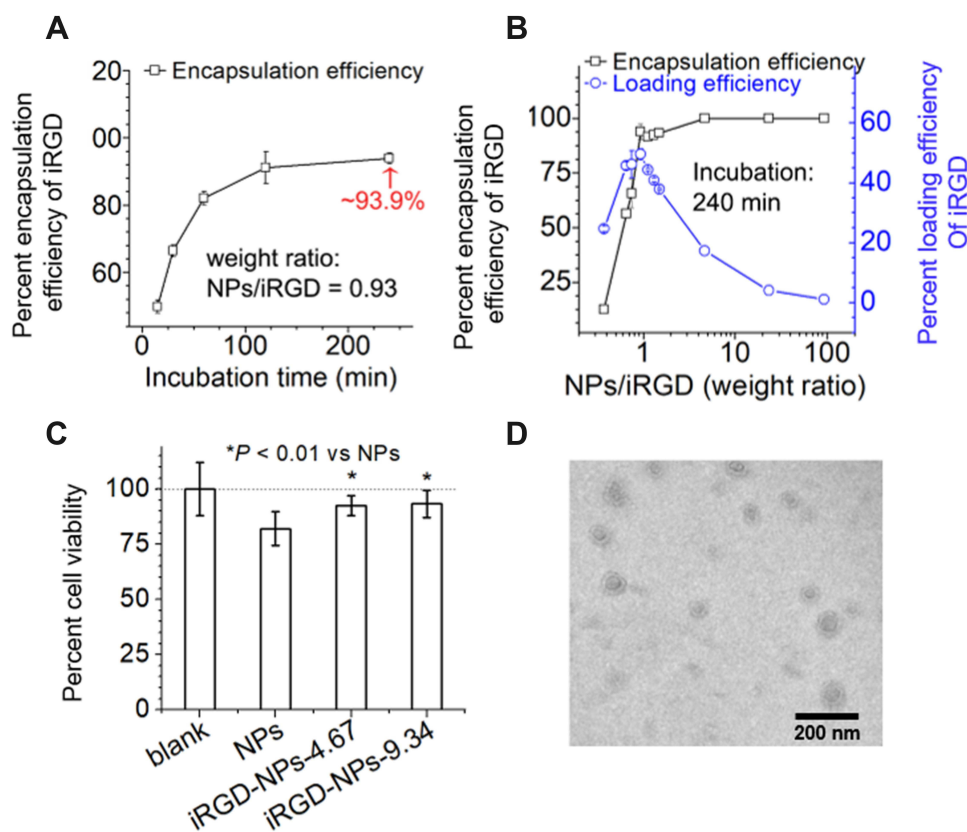


Figure 1 Preparation and characterization of iRGD-NPs. Loading capacity of LPSA nanopolymersomes (NPs) to iRGD: effects of incubation time (**A**) and weight ratio of NPs/iRGD (**B**) on iRGD loading. (**C**) Cytotoxicity of iRGD-NPs to rMSCs, where iRGD-NPs with different NPs/iRGD weight ratios contain 35 $\mu\text{g}/\text{mL}$ NPs (final concentration in culture media). (**D**) TEM image of iRGD-NPs-9.34.

ratio of 0.93 (NPs/iRGD, *W/W*). It should be noted that we used weight ratio for all preparation recipes unless otherwise stated. The encapsulation efficiency (EE) of iRGD increases with incubation time, at 15 min, the EE is ~50%, and at 240 min, the value reaches ~94%, suggesting that NPs have high iRGD-capturing capacity. Thereafter, with incubation time of 240 min, we studied the effects of weight ratio of NPs/iRGD on iRGD encapsulation (**Figure 1B**). It can be seen that, the EE increases with the weight ratio of NPs/iRGD, at NPs/iRGD ≥ 0.93 , the EE is $>90\%$, and at NPs/iRGD ≥ 4.67 , the EE reaches 100%. Correspondingly, with an increase of NPs/iRGD, the loading efficiency (LE) of iRGD gradually increases to its apex at NPs/iRGD ≈ 0.93 , and then decreases. These results suggest that NPs have excellent iRGD-capturing capability through electrostatic, hydrogen-bond and hydrophobic interactions. Meanwhile, the loading of iRGD can be controlled by incubation time and weight feeding ratio of NPs/iRGD. Based on these data, we conclude that iRGD-NPs should be prepared at NPs/iRGD ≥ 4.67 with incubation time of 240 minutes, and the optimal weight ratio of NPs/iRGD should be further explored by in vitro and in vivo transfection experiments. The reasons are as follows.

Firstly, for cost control, it is reasonable to maximize EE because iRGD is very expensive. Secondly, in our system, iRGD acts as a functional ligand for improving the tumor targeting and penetration of nanopolymersomes rather than a therapeutic drug, and therefore on the premise of ensuring efficient tumor targeting and penetration of iRGD-NPs, LE of iRGD should be minimized. Thirdly, positive charges of PEI and iRGD on NPs surfaces both contribute to the transfection efficiency.²² The former improves the transfection efficiency through the following ways: the positive charge mediates the attractive interactions between cationic NPs and anionic cell/endosomal membranes, which facilitates cell binding and subsequent endocytosis, and promotes the endosomal escape and the release of nano-delivery system into the cytoplasm due to proton sponge effect. The latter improves the transfection efficiency by iRGD-receptor mediated endocytosis and tumor tissue penetration. However, the introduction of iRGD on NPs surfaces shields/reduces the positive charges, and furthermore, excessive iRGD may shield the binding of iRGD receptor on cell surfaces due to the

lateral steric hindrance of iRGD, both of which decrease the transfection. Additionally, it is reported that in some cases, the enhancement of transfection efficiency mediated by positive charges overpowers the one by receptor.²² Finally, there is a limiting level of iRGD-receptor-mediated cellular uptake and penetration due to the limited number of iRGD receptors on cell membranes and steric hindrance. Therefore, optimizing the amount of decorated iRGD is important to improve the antitumor therapeutic efficacy rather than “the more, the better”. In other words, it is optimal to maximize the therapy efficacy at minimal cost by introducing the least amount of iRGD onto siRNA/iRGD-NPs.

Cytotoxicity of iRGD-Functionalized Lipopolysaccharide-Amine Nanopolymersomes to Mesenchymal Stem Cells

The ideal anti-cancer drug delivery vectors should be low toxic to normal somatic cells, while able to target cancer-related cells, and then release the cargoes to kill them. We have demonstrated that the toxicity of NPs and gene-loaded NPs to rMSCs and zebrafish is low,^{13–16} and we infer that introducing iRGD onto NPs may further improve the cytocompatibility. Via AlamarBlue method using rMSCs as a somatic model cell, the cytotoxicity of iRGD-NPs containing 35 µg/mL NPs (final concentration in culture media) with different NPs/iRGD weight ratios was evaluated, and results were presented in **Figure 1C**. As expected, after treated by iRGD-NPs for 48 h, the cell viability of rMSCs is >90%, which is higher than that treated by NPs, indicating that iRGD modification does reduce the cytotoxicity of NPs. Such decrease in cytotoxicity of iRGD-NPs is possibly attributed to the excellent compatibility of iRGD, a drop in positive charge density on iRGD-NPs surfaces, and a reduction in nonspecific binding of vectors to cells. It is well known that the positive charge of cationic vectors for siRNA delivery is one of the key sources of cytotoxicity.^{13,15,22–24} For example, for PEI-based vectors, their positive charges mediate the nonspecific binding of vectors to anionic cell membranes through electrostatic interactions, which may induce membrane destabilization and a loss of membrane integrity due to the possible aggregation of vectors on cell surfaces, and thus leads to cytotoxicity. iRGD decoration decreases the overall positive charge density of NPs with PEI corona, which is confirmed by the drop in the zeta potential after modification (42.4 mV for NPs, 24 mV for iRGD-NPs), and is realized in two ways. The one is via charge neutralization between positively charged PEI and negatively charged iRGD. The other is via shielding the exposure of positive charges due to the lateral steric hindrance of iRGD.²² Furthermore, iRGD decoration decreases the nonspecific cell binding mediated by positive charges of vectors, possibly reducing the above-mentioned related cytotoxicity.

Such a decrease in toxicity to normal somatic cells is welcome for nucleic acids-delivery systems. Interestingly, in our studied range, for the same concentration of NPs (35 µg/mL) in iRGD-NPs, higher iRGD concentration in iRGD-NPs does not always cause a significant improvement of cytocompatibility: the cell viability for iRGD-NPs-4.67 containing 7.49 µg/mL iRGD and iRGD-NPs-9.34 containing 3.75 µg/mL iRGD is 92.5% and 93.3%, respectively, suggesting that more iRGD does not necessarily bring about positive returns. Considering the cost, minimizing the introduction of chemicals into body, and minimizing the iRGD introduction but maximizing the tumor-targeting/-penetrating ability of delivery system (discussed below), iRGD-NPs-9 might be a good choice as a target vector for in vitro cell transfection.

TEM Observation on iRGD-Functionalized Lipopolysaccharide-Amine Nanopolymersomes

We observed the morphology of iRGD-NPs-9 using TEM (**Figure 1D**). Similar to NPs,¹³ iRGD-NPs-9 still take the spherical nanopolymersomes morphology with a diameter of ~80 nm, which is slightly larger than NPs (diameter ~70 nm) due to iRGD decoration. ~80 nm is lower than its hydrodynamic diameter (123 nm, measured by DLS) due to the dry vacuum state in TEM observation.

Stability of iRGD-Functionalized Lipopolysaccharide-Amine Nanopolymersomes in Different Environments

We evaluated the storage stability by monitoring the changes in the size and zeta potential of lyophilized iRGD-NPs-9 at 4°C with time. After stored at 4°C for one year, the size of iRGD-NPs keeps unchanged (**Figure 2A**), and the zeta potential changes slightly from 28.2 ± 5.4 mV to 32.1 ± 3.0 mV, suggesting their storage stability in this condition. Next, the stability of iRGD-NPs in PBS

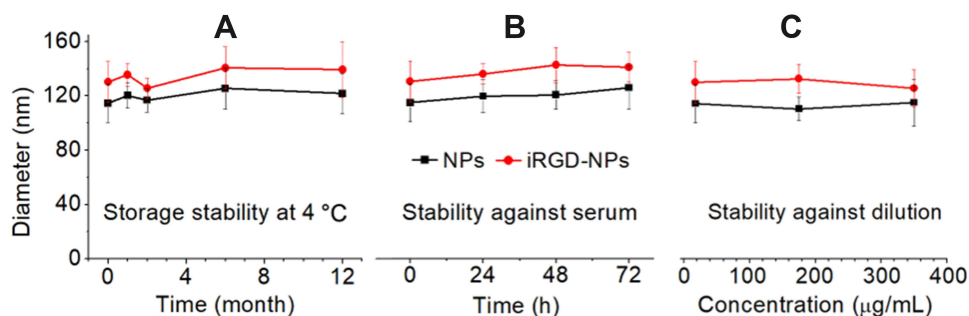


Figure 2 Size stability of iRGD-NPs in different environments. (A) Storage stability of lyophilized iRGD-NPs at 4°C with time. (B) Stability of iRGD-NPs against serum. (C) Stability of iRGD-NPs against dilution.

containing 20% serum was evaluated (Figure 2B). Our results show that in 72 h, the size of iRGD-NPs keeps unchanged, indicating that iRGD modification does not change the ability of NPs in short-term anti-aggregation induced by serum proteins,¹⁵ which is important for efficient transfection. Then, we studied the stability of iRGD-NPs against dilution because the first barrier for gene-delivery vectors in vivo is massive hemodilution. Similar to NPs,¹⁵ iRGD-NPs is able to resist dilution, and their size remained stable at ~130 nm in the range of 350 µg/mL to 17.5 µg/mL (Figure 2C). We believe such anti-dilution capability of iRGD-NPs provides the feasibility for their in vivo application as a siRNA delivery vector, because after hemodilution, the final concentration of iRGD-NPs in the blood circulation is ~70 µg/mL, which just locates in the abovementioned dilution-tolerance concentration range. Notably, the concentration of ~70 µg/mL was deduced as follows. In general, for in vivo gene therapy such as in mice, the suggested dosage for siRNA is 0.5 mg/kg per intravenous injection and the suggested weight ratio of nanodelivery vector to siRNA is 10,¹⁸ the circulating blood volume is 1.8 mL for 25 g of mice, and as a result, the final concentration of nanovector is estimated as ~70 µg/mL. Additionally, the critical aggregation concentration of lipopolysaccharide (LPSA) and gene-loaded LPSA nanoparticles is 1.38 µg/mL (determined by pyrene fluorescence probe technique)¹³ and 1.95 µg/mL (determined by surface tension method),¹⁵ respectively, further ensuring the stability of iRGD-NPs nanopolymersomes in blood circulation.

Preparation and Characterization of siVEGF-Loaded Lipopolysaccharide-Amine Nanopolymersomes Functionalized with iRGD

siRNA/iRGD-NPs was prepared by successively incubating NPs with siRNA and iRGD, where the weight feeding ratio was set as NPs/iRGD/siRNA=9/1/1. We chose such preparation conditions due to the following reasons: 1) siRNA can be completely retarded at NPs/siRNA ≥ 1.25 (Figure S2), 2) the 100% of EE is achieved at NPs/iRGD ≥ 4.67 (Figure 1A and B), 3) the good cytocompatibility of iRGD-NPs containing 35 µg/mL with weight ratio of NPs/iRGD = 4.67–9.34 (Figure 1C), 4) the optimal transfection of siRNA/NPs is achieved at NPs/siRNA = 5.03 according to our previous study,¹⁴ 5) the suggested weight ratio of nanodelivery vector to siRNA is 10,^{18,20} 6) iRGD and siRNA is expensive. As expected, siRNA/iRGD-NPs with this weight ratio have achieved excellent in vitro and in vivo transfection effects, which will be presented below. The as-prepared siRNA/iRGD-NPs were characterized by TEM and DLS. Observation by TEM visually proves that siRNA/iRGD-NPs keep nanopolymersomes structure (Figure 3A), which is similar to NPs,¹³ and such nanopolymersomes structure is believed to be beneficial for endocytosis due to the similarity to cell membranes. DLS assay shows that the hydrodynamic diameter and zeta potential of siRNA/iRGD-NPs is ~130 nm and ~-33.5 mV, which is slightly different from that of NPs (~114 nm, ~-40 mV), and such difference is possibly attributed to the surface decoration of cyclic iRGD with weakly negative charges. It is worth noting that the diameter of nanopolymersomes just locates in the range of 30–200 nm, which is believed to be ideal for systemic in vivo delivery as they can avoid rapid renal clearance and remain in circulation.¹⁸

Tumor Cell Selection

Results of WesternBlot analysis show that, MCF-7 expresses maximum receptors of $\alpha_v\beta_3$ integrin and NPR-1 among 293T, 293FT, MCF-7, and Hela cells (Figure S3), suggesting that MCF-7 is appropriate as a target cell model. Thus, we chose MCF-7 for siRNA-delivery experiments in this study.

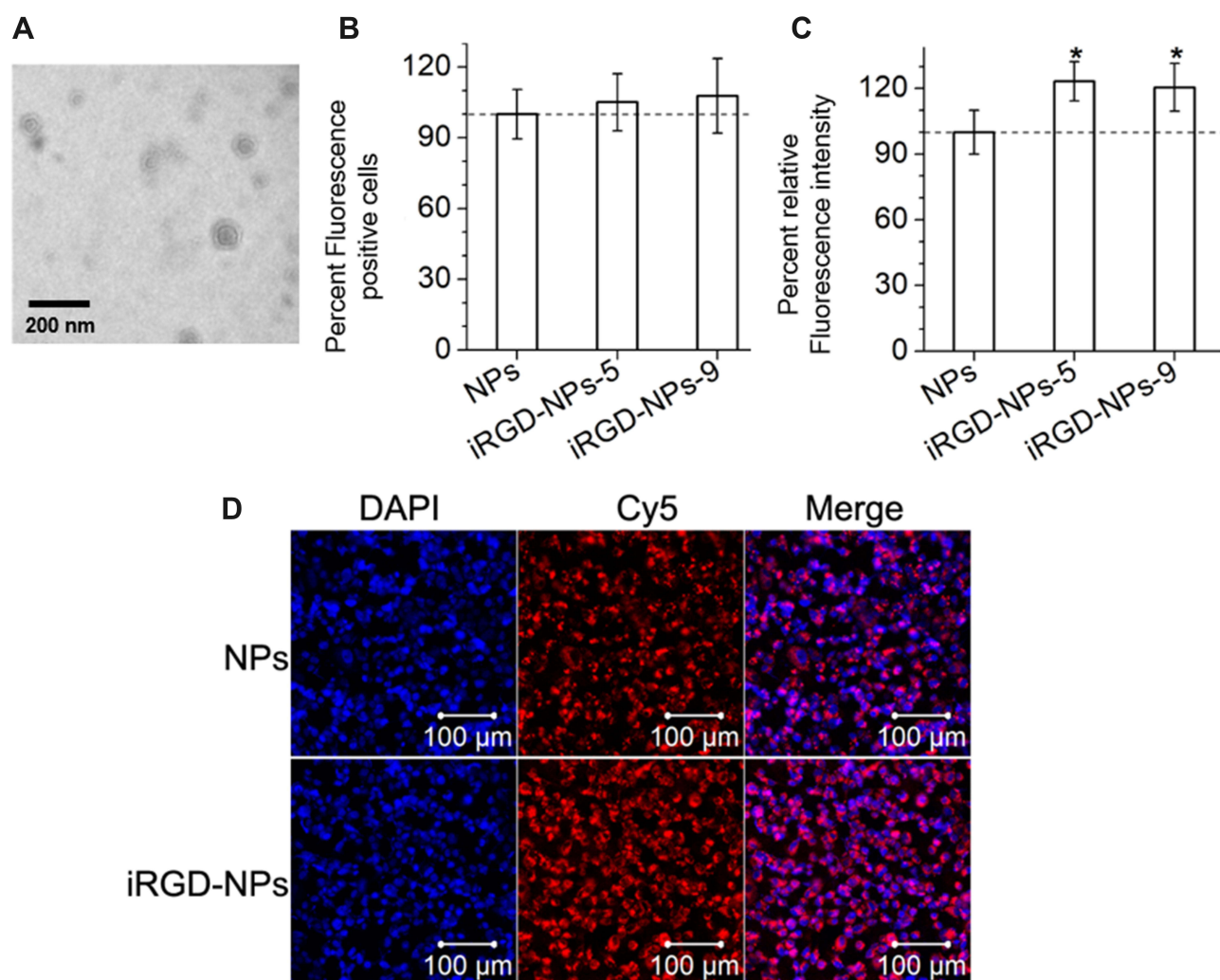


Figure 3 Preparation and characterization of siRNA/iRGD-NPs. **(A)** TEM image of siRNA/iRGD-NPs with a weight feeding ratio of NPs/iRGD/siRNA = 9/1/1 and a final concentration of siRNA at 50 nM. Cellular uptake of MCF-7 to siRNA/iRGD-NPs after coinubation for 240 mins: **(B)** relative transfection efficiency and **(C)** relative average fluorescence intensity analyzed by flow cytometer. **(D)** Images of MCF-7 treated by siRNA/iRGD-NPs under laser confocal scanning microscope. The fluorescence signal of siRNA (labeled by Cy5) is red, and cell nuclei (labeled by DAPI) is blue, respectively. * $P < 0.01$ vs NPs.

The Introduced iRGD Facilitates the Cellular Uptake of siRNA by MCF-7 Cells

Firstly, we investigated the effects of incubation time on cellular uptake by incubating MCF-7 with Cy5-siRNA-loaded iRGD-NPS for different time using laser confocal scanning microscope and flow cytometry. As shown in [Figure 3](#) and [S4](#), the cellular uptake of Cy5-siRNA-loaded iRGD-NPs increases with incubation time, and reaches ~100% at 240 min, which is consistent with our previous study on cell uptake of gene-loaded NPs.^{13,14,16} Therefore, we chose 240 min for all transfection experiments unless otherwise stated.

Secondly, to evaluate the targeting ability of introduced iRGD to MCF-7, we analyzed the cellular uptake behavior of Cy5-siRNA/NPs and Cy5-siRNA/iRGD-NPs with different iRGD concentrations ([Figure 3B–D](#)). It is interesting that, although the relative average fluorescence intensity for iRGD-NPs system is higher than that for NPs system, there is no significant difference in the percentage of fluorescence-positive cells between two groups. Such result can be explained by the efficient cytosolic delivery capability of NPs with ~100% transfection efficiency,¹³ which means that Cy5-siRNA-loaded nanopolymersomes enter into almost all cells, but the amount entering into cells varies. Obviously, iRGD has enhanced this entry, confirming that the introduced iRGD still has its tumor cell targeting bioactivity. In addition, the relative average fluorescence intensity for siRNA/iRGD-NPs-9 group is almost the same as that for siRNA/iRGD-NPs-5 group, although the latter has more iRGD on NPs surfaces. This result again confirms that 9/1 may be an appropriate

weight ratio of NPs to iRGD for an efficient siRNA delivery, suggesting that introducing iRGD on NPs is not “the more the better”. Because this paper focuses on the loading capacity of NPs to iRGD via self-assembly method and the corresponding activities of introduced iRGD in tumor-targeting and penetrating delivery of siRNA, we have not tried lower iRGD concentration (higher weight ratio of NPs/iRGD), which may be further studied in the future. Nonetheless, from these results, we can conclude that introducing iRGD to NPs by this self-assembly method does enhance the cancer cell-targeting delivery.

Endocytosis Pathway of siRNA-Loaded Lipopolysaccharide-Amine Nanopolymersomes Functionalized with iRGD in Tumor Cells

To reveal the mechanism in the enhanced cellular uptake of iRGD-NPs by MCF-7, we studied the endocytosis pathway in MCF-7 by using six inhibitors including iRGD, anti-ApoER2, sodium azide, Genistein, Amiloride-HCl, and Amantadine. Our results show that the average fluorescence intensity relative to the control (%AFI) decreases in varying degrees in all inhibitor groups (Figure 4), indicating that multiple pathways are involved in endocytosis of Cy5-siRNA/iRGD-NPs with different contributions. Specifically, for the group pretreated by iRGD, %AFI significantly decreases to 67%, indicating that the iRGD receptor-mediated endocytosis pathway is involved in this delivery system, and the grafted iRGD on NPs can specifically bind to MCF-7 to enhance the endocytosis. Additionally, lipoprotein receptor-mediated endocytosis is verified for iRGD-NPs delivery system, where %AFI decreases by ~21% for the group pre-treated by anti-ApoER2, which is induced by cholesterol block in NPs as our previous report.¹³ Besides receptor-mediated endocytosis, we tested other pervasive endocytosis pathways. For example, when MCF-7 were pretreated by Sodium Azide, %AFI decreases to 40.48%, indicating the energy-dependent endocytosis of this system; for groups treated by Genistein, Amiloride-HCl, and Amantadine, %AFI decreases to 35%, 51%, and 78%, respectively, suggesting that cave protein-, micropinocytosis-, and clathrin-mediated endocytosis were also involved. In short, these results support that at least five pathways are involved in endocytosis of siRNA/iRGD-NPs by MCF-7, and just as designed, iRGD-acceptor-mediated endocytosis plays an important role, which may realize efficient tumor targeting of iRGD-NPs. This result also explains the above cellular uptake data with almost the same transfection efficiency but increased fluorescence intensity.

iRGD-Functionalized Lipopolysaccharide-Amine Nanopolymersomes Enhance the Tumor Spheroid Penetration of siRNA

After testing the tumor-targeting ability of siRNA/iRGD-NPs, the in vitro tumor-penetration ability of this system was explored using a tumor spheroid model. We first determined the optimal conditions (including cell concentration in hanging drops, and the culture time on inverted lids and on agar) for preparing MCF-7 spheroids. Our results show that (Figure S5), the 5–50k cells/drop for 48 hours' culture on inverted lids and 96 hours' culture on agar can successfully

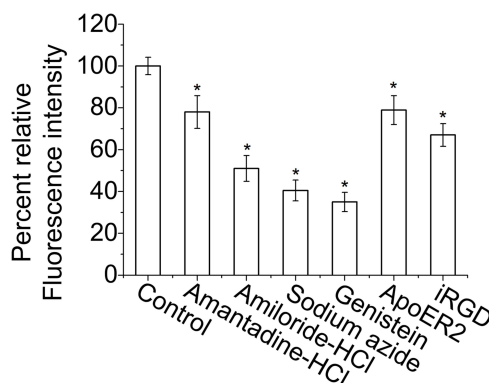


Figure 4 Endocytosis pathway of Cy5-siRNA/iRGD-NPs-9 in MCF-7. MCF-7 were pre-incubated with inhibitors including iRGD, anti-ApoER2, Sodium azide, Genistein, Amiloride-HCl, and Amantadine for 1 h, followed by 1 hour's incubation with Cy5-siRNA/iRGD-NPs-9. * $P < 0.05$ vs Control.

produce dense three-dimensional tumor spheroids with a diameter of $\sim 1000 \mu\text{m}$, and the detailed information on tumor spheroid preparation was presented in [Figure S5](#).

The penetration experiment for two nanopolymerosomes systems of siRNA/iRGD-NPs and siRNA/NPs was performed on tumor spheroids with a diameter of $\sim 1000 \mu\text{m}$, and the results were presented in [Figure 5](#). As expected, both systems have the ability to penetrate tumor spheroids, and their fluorescence intensity (FI) gradually decreases due to the diffusion limitation, but the FI for siRNA/iRGD-NPs group is always higher than that for siRNA/NPs group at the same penetration depth ([Figure 5A and B](#)), and their FI ratio ranges from 1.2 to 2.7 ([Figure 5C](#)). With an increase of penetration depth, the FI ratio of two groups gradually increases to the maximum of 2.7 at $250 \mu\text{m}$, and then decreases to 1.2 at $400 \mu\text{m}$. Such trend is reasonable due to the diffusion limitation and relatively short incubation time of 4 hours, proving the efficient cytosolic delivery ability of NPs, and the introduced iRGD on NPs still preserves its tumor-targeting and penetration ability, thus significantly enhancing the penetration of siRNA/iRGD-NPs to tumor tissue compared to siRNA/NPs.

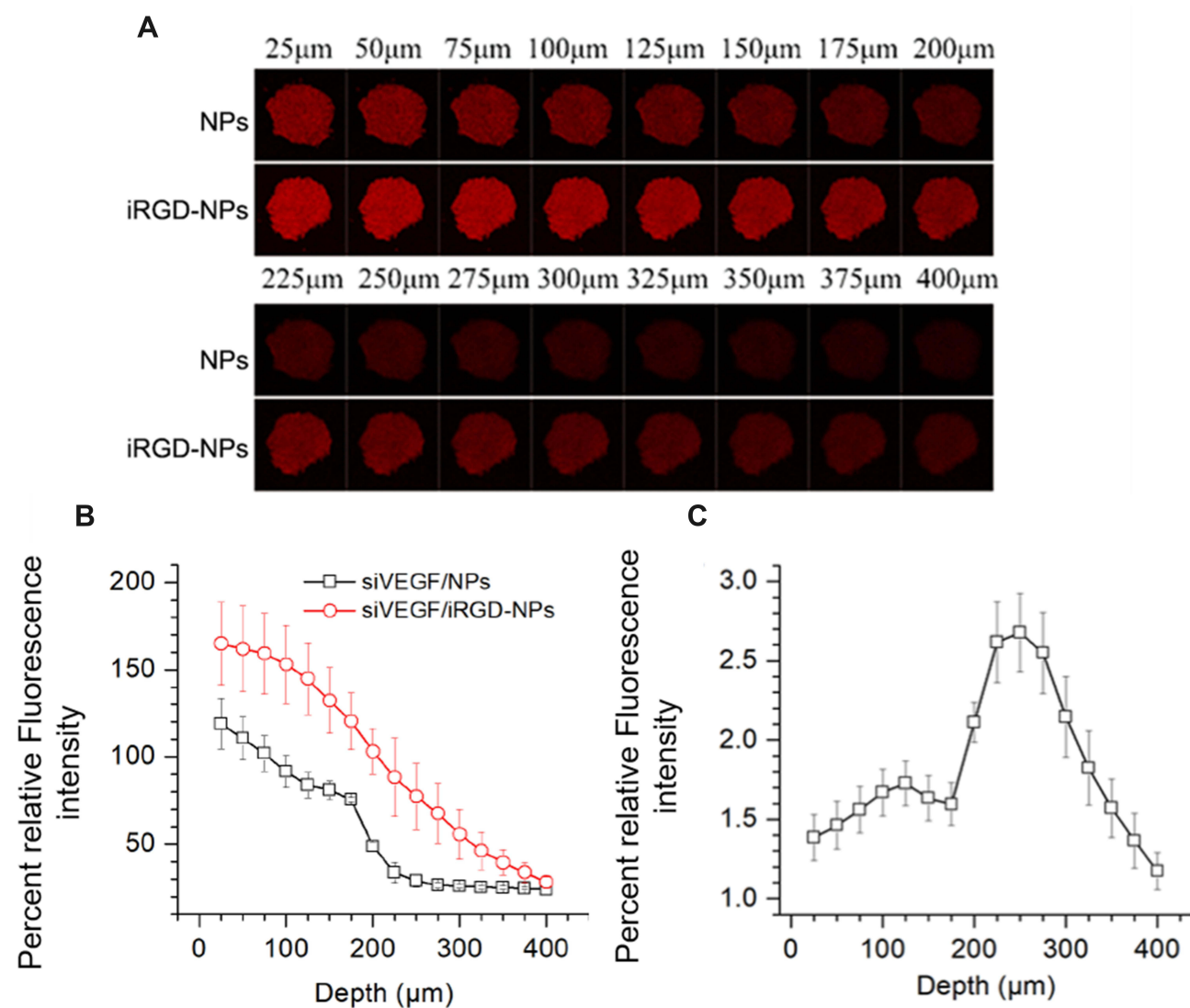


Figure 5 Targeted penetration of Cy5-siRNA-loaded iRGD-NPs or NPs into MCF-7 spheroids. **(A)** Scanned images of tumor spheroids. Pictures were taken with laser confocal microscopy from the top to the middle of spheroids per $25 \mu\text{m}$. **(B)** Relative fluorescence intensity of scanned images in **(A)**, analyzed by ImageJ software. **(C)** Ratio of fluorescence intensity of Cy5-siRNA/iRGD-NPs to Cy5-siRNA/NPs at the same depth.

iRGD-Functionalized Lipopolysaccharide-Amine Nanopolymersomes Improve the Anti-Angiogenesis of *siVEGF* in Zebrafish

An in vivo anti-angiogenesis experiment was performed on transgenic zebrafish. The optimal concentration of NPs for in vivo *siVEGF* delivery was first explored. In our studied range, the toxicity (survival rate) and anti-angiogenesis induced by NPs is dose-dependent without significantly affecting the development and growth of zebrafish. As shown in [Figure S6](#), with NPs concentration increases, the survival rate of zebrafish treated by *siVEGF*/NPs decreases. However, even at 50 $\mu\text{g/mL}$ of NPs in culture media, zebrafish still has a survival rate of 78.89%, suggesting that *siVEGF*/NPs may be suitable for in vivo application. For anti-angiogenesis, the length and area of SIV in zebrafish decrease with the increase of NPs concentration. Specifically, when the final concentration of NPs in culture media is 25, 33.5, and 50 $\mu\text{g/mL}$, the average length of SIV for *siVEGF*/NPs groups is 0.76, 0.53, and 0.43 of that for the blank group, and the corresponding area is 0.57, 0.53, and 0.43 of that for the blank group, respectively. Based on these results, we believe that 50 $\mu\text{g/mL}$ of NPs (final concentration) is an optimal concentration for in vivo *siVEGF* delivery in zebrafish, which guarantees significant anti-angiogenesis with acceptable survival rate.

To obtain an optimal concentration of iRGD for in vivo application in zebrafish, we first studied the effects of *siVEGF*/iRGD-NPs on growth and development of zebrafish by changing iRGD concentration but fixing the concentration of NPs (50 $\mu\text{g/mL}$) and *siVEGF* (50 nM) ([Figure 6A and B](#)). The results reveal that for zebrafish treated by *siVEGF*/iRGD-NPs, with an increase in iRGD concentration in culture media, their vessel length/area of SIV and survival rate decrease. When the iRGD concentration in culture media is 10 and 20 $\mu\text{g/mL}$, zebrafish grow malformed or die in the embryonic stage ([Figure 6Ae and Af](#)), and their survival rate is lower than 70%. We speculated that iRGD decoration on NPs could specifically and efficiently deliver *siVEGF* to zebrafish neovascularization rich in iRGD receptors of $\alpha_v\beta$ integrins, then specifically silence VEGF gene, and effectively inhibit the angiogenesis, thus leading to malformation or death of zebrafish due to defects in circulation system. Based on these results, to avoid death, we chose the final concentration of iRGD in culture media <10 $\mu\text{g/mL}$ to evaluate the anti-angiogenic efficacy of *siVEGF*/iRGD-NPs.

As we hypothesized, with an increase in iRGD concentration, the angiogenesis decreases, and such decrease was verified by the reduction in the length and area of SIV in zebrafish treated by *siVEGF*/iRGD-NPs for 48 h ([Figure 6C](#)). For *siVEGF*/iRGD-NPs groups, when the final concentration of iRGD in culture media is 0, 2.5, and 5 $\mu\text{g/mL}$ (corresponding to *siVEGF*/iRGD-NPs-0, *siVEGF*/iRGD-NPs-20, and *siVEGF*/iRGD-NPs-100), their average length of SIV is 62%, 52%, and 41% of that for the blank group, and the corresponding area is 42%, 37%, and 21% of that for the blank group, respectively. Compared with *siVEGF*/NPs, the anti-angiogenesis induced by *siVEGF*/iRGD-NPs-20 and *siVEGF*/iRGD-NPs-10 was enhanced by 1.19 and 1.51 folds (length of SIV), and 1.14 and 2.00 folds (area of SIV), respectively. These results demonstrate that the decoration of iRGD on NPs enhances the anti-angiogenesis significantly in zebrafish. Such enhancement is attributed to the synergic effects from neovascularization targeting induced by iRGD, and subsequent efficient VEGF gene silencing induced by *siVEGF*. It is worth noting that in MCF-7, iRGD concentration in NPs-iRGD did not significantly affect the cellular uptake ([Figure 3](#)), but in zebrafish, higher iRGD concentration leads to the stronger anti-angiogenesis, which may be ascribed to the lower level of $\alpha_v\beta_{3/5}$ on MCF-7 surfaces than that on neovascular cell surfaces in embryonic zebrafish.

iRGD-Functionalized Lipopolysaccharide-Amine Nanopolymersomes Increase the Gene Silencing Efficiency of *siVEGF* in Zebrafish

To disclose the mechanism of anti-angiogenesis of *siVEGF*/iRGD-NPs in zebrafish, we further used qRT-PCR to quantify the VEGF mRNA level in zebrafish. As shown in [Figure 7](#), increasing iRGD concentration weakens the expression of VEGF mRNA in zebrafish in our studied range. The relative expression level of VEGF mRNA in groups of *siVEGF*/NPs, *siVEGF*/iRGD-NPs containing 2.5 and 5.0 $\mu\text{g/mL}$ iRGD in culture media are 73%, 67% and 42% of that in blank group, respectively. These results confirm that *siVEGF*/iRGD-NPs can target zebrafish neovascularization and specifically silence VEGF gene, thus inhibiting angiogenesis in zebrafish, which is consistent with the inhibition of *siVEGF*/iRGD-NPs on the length and area of SIV in zebrafish.

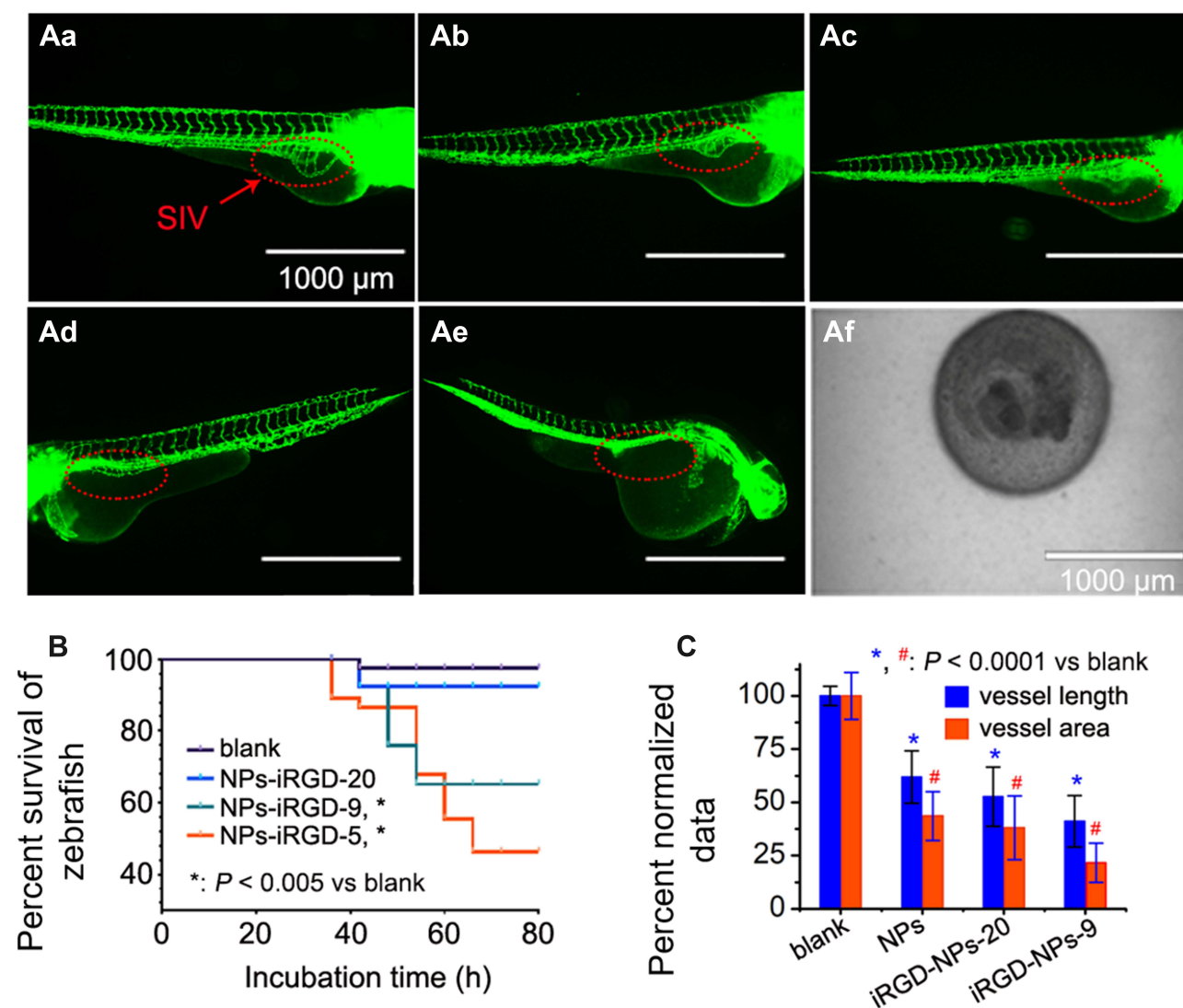


Figure 6 In vivo anti-angiogenesis performance of siVEGF/iRGD-NPs. Zebrafish at 24 hpf were treated by siVEGF/iRGD-NPs with different concentrations of iRGD for 48 h. (Aa–Af) images of zebrafish untreated (Aa), or treated by siVEGF/iRGD-NPs containing 0, 2.5, 5, 10, and 20 $\mu\text{g}/\text{mL}$ iRGD in culture media, respectively (Ab–Af). (B) Kaplan–Meier survival curves of zebrafish treated by siVEGF/iRGD-NPs for 80 h. (C) Vessel length and area of SIV in zebrafish treated by siVEGF/iRGD-NPs for 48 h. All concentrations here referred to the final concentration in culture media. 50 nM siVEGF and 50 $\mu\text{g}/\text{mL}$ NPs were used for siVEGF/iRGD-NPs groups. Untreated zebrafish (blank) was used as a control. Scale bar: 1000 μm .

siVEGF-Loaded Lipopolysaccharide-Amine Nanopolymerosomes Functionalized with iRGD Inhibit the Tumor Growth and Decrease VEGF Protein Level in Mice

To evaluate the in vivo antitumor effects of siVEGF/iRGD-NPs, they were intravenously injected into mice bearing tumor, then the mice weight, tumor volume, and the VEGF protein level in tumor tissues were measured at designed time points, and saline along with siVEGF/NPs were used as controls. The results show that siVEGF/iRGD-NPs have enhanced anti-tumor activity with relative lower toxicity when compared with siVEGF/NPs and saline (Figure 8). After administration, mice showed no abnormalities and deaths. The mice weight increases in all three groups, but the weight in saline group increases more slowly, and the order of mice weight is saline group < siVEGF/NPs group < siVEGF/iRGD-NPs-9 group (Figure 8B). Such difference possibly suggests the low toxicity of nanomedicine, whose adverse effects are lower than that caused by tumor itself.

The anti-tumor effects of nanomedicine were evaluated by the changes in tumor volume relative to the saline group after drug treatment. Figure 8C shows that, siVEGF/iRGD-NPs has a significant anti-tumor efficacy, which is more powerful than siVEGF/NPs: on day 14 post administration, the inhibition rate of tumor growth reaches 66.79% for

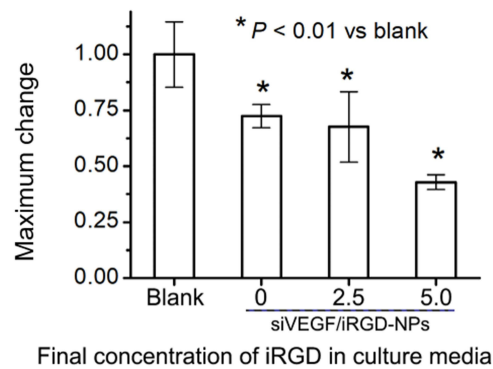


Figure 7 Expression of VEGF mRNA in zebrafish treated by siVEGF/iRGD-NPs with different iRGD concentrations. Untreated zebrafish (blank) was used as a control.

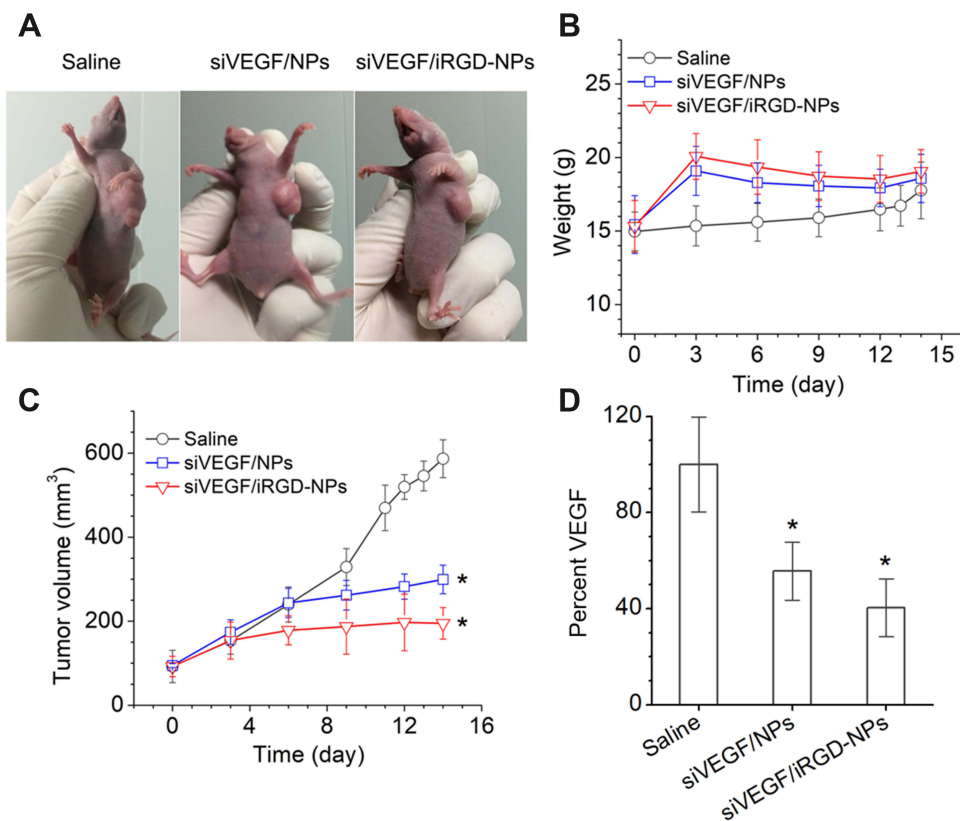


Figure 8 Antitumor effects of different siVEGF-delivery systems in nude mice bearing breast cancer via intravenous administration. (A) Images of mice on day 14 post administration. (B) Changes of animal weight with time. (C) Changes of tumor volume with time, * $P < 0.01$ vs saline only for data on day 14. (D) Relative VEGF protein level in tumor tissues (data from ELISA), * $P < 0.01$ vs saline. $n = 5$.

siVEGF/iRGD-NPs and 48.96% for *siVEGF/NPs*, respectively. Furthermore, to elucidate the mechanism of nanomedicine in inhibiting tumor growth, we measured the VEGF protein level in tumor tissues. As expected, the VEGF level in tumor tissues was significantly reduced by the nanomedicine (Figure 8D). The expression of VEGF protein in *siVEGF/iRGD-NPs* group drops to 40% of that in saline group, and the value is 56% in *siVEGF/NPs* group. This is consistent with the results in tumor volume, demonstrating that *siVEGF* can be efficiently delivered into the tumor tissue by iRGD-NPs or NPs, then silence the VEGF gene to down-regulate the expression of VEGF protein, thus inhibit the angiogenesis, and finally inhibit the tumor growth. Such anti-cancer efficacy is significantly enhanced by iRGD-NPs, confirming that

the iRGD introduced by a physical self-assembly method can endow the siRNA delivery system with efficient tumor-targeting and penetrating ability.

Discussion

Cancer is a serious global health problem, and a therapy with high efficiency and low toxicity is the ultimate goal for cancer treatment. Small interfering RNA (siRNA) has been demonstrated to be a promising therapeutic agent for cancer.^{1–3,25} However, as biomacromolecules with negative charges, siRNAs cannot be used directly in vivo because they are easily degraded and quickly eliminated during in vivo circulation, and they cannot reach and enter the target cancer tissues and cells to function by themselves. Therefore, safe, efficient, specific, and non-pathogenic delivery vectors are urgently needed to ferry siRNAs into target tissue and cells. Although a lot of delivery vectors have been developed for siRNA delivery in two decades, the ones that fully meet clinical requirements are still not available.^{1–3,25} Ideal vectors for siRNA delivery should overcome the biological obstacles during in vivo delivery procedure, which consists of five cascade steps of *CAPIR* for intravenous administration: circulation, accumulation, penetration, internalization, and release.^{3,26} Nanomaterials can be engineered to surmount those biological barriers via introducing various functional components, and thus offer unlimited potential in siRNA delivery. So far, many nanomaterial delivery systems exhibit excellently in C, I, and R steps, but their poor performance in step A of tumor accumulation and step P of tumor penetration hampers the overall therapeutic efficacy.^{1,2,25,26} To solve this problem, in this study, we used iRGD, a cancer-targeting/penetrating peptide to decorate LPSA nanopolymersomes to deliver siRNA for cancer-target treatments. Different from the complicated covalent coupling method generally used for iRGD introduction into nano-vectors for target therapy, we decorated nanopolymersomes via a facile physical method of self-assembly in water between nanopolymersomes and iRGD to enhance the tumor accumulation and penetration of siRNA.

Theoretically, LPSA nanopolymersomes (NPs) have the ability to load iRGD possibly via physical interactions (such as electrostatic interactions, hydrophobic interactions, and hydrogen bonds), because both LPSA and iRGD are amphiphilic and amphoteric (Figure S1B). iRGD is a cyclic peptide with 9 amino acid sequences (CRGDKGPDC) (Figure S1B). Although iRGD has 3 free carboxyl residues, 2 free amine residues, and 1 guanidine group, it is negatively charged at pH >5.02 (the isoelectric point of cysteine) because the free -NH₂ in cysteine (C) is not protonated. As mentioned in introduction, NPs have a membrane composed of cholesterol and OA/PEI complexes surrounded by PEI coronas (Figure S1B),¹³ and we have demonstrated that NPs are stable with polymersomes structure at pH 3.4–10.4, and they are positively charged at pH <10.1 and with zeta potential >30 mV at pH ≤8.¹⁵ Therefore, in theory, there exist electrostatic interactions between NPs and iRGD at pH > ~5. Additionally, iRGD may interact with NPs by hydrophobic interactions and hydrogen bonds due to the amphiphilicity and amphotericity of LPSA and iRGD. Based on these, we conclude that NPs can form a stable complex with iRGD by aforementioned interactions at pH > ~5, which may guarantee iRGD-NPs against disassembly/disassociation due to pH changes in different physiological environments during service. The reason is that, for siRNA delivery vectors for anti-tumor therapy, since the pH is ~7.4 in blood and cytosol, ~6.8 in tumor tissue, ~8 in intestine, and ~5.0–6.5 in endosome, the in vivo environmental pH encountered by them is > ~5. Thus, the concerns over disassembly/disassociation of iRGD-NPs in physiological environments for self-assembled nanodelivery vectors driven by pH-dependent non-covalent interactions (such as electrostatic interactions, hydrophobic interactions and hydrogen bonds) may be addressed. Furthermore, we have demonstrated that NPs have efficient cytosolic delivery ability due to efficient endocytosis and endosome escape, and can efficiently deliver pDNA/siRNA into cells/zebrafish to induce/silence the expression of target genes without obvious cytotoxicity.^{13,15,16} Therefore, we believe that LPSA nanopolymersomes are capable of loading iRGD by co-incubation, and the as-prepared iRGD-NPs can efficiently deliver siRNA for enhanced anti-tumor therapy due to the active tumor-targeting and penetration ability conferred by iRGD.

Our results have confirmed these. After sequential co-incubation of LPSA first with *siVEGF* and then with iRGD in water, both siRNA and iRGD were efficiently complexed by LPSA NPs to form siRNA-loaded LPSA nanopolymersomes decorated with iRGD (siRNA/iRGD-NPs), which was evidenced by gel electrophoresis, micro-BCA assay, DLS, and TEM observation (Figures 1–2). iRGD decoration improved the cytocompatibility of NPs (Figure 1C). The introduced iRGD onto NPs via a physical method of self-assembly still possesses high affinity to α_vβ integrins and NPR-1 receptor which were highly expressed on tumor neovascular cells and tumor cells, and thus endow siRNA/iRGD-

NPs with tumor-target and penetration ability. We first choose MCF-7 as a tumor model cell to test the target function of decorated iRGD. As shown in Figures 3 and 4, compared to siRNA/NPs, siRNA/iRGD-NPs has enhanced cellular uptake by MCF-7 induced by iRGD receptor-mediated endocytosis. Similarly, the tumor-penetration ability of siRNA/iRGD-NPs in MCF-7 spheroids was enhanced by 2.7-fold compared to that of siRNA/NPs (Figure 5). Thereafter, using a zebrafish embryo model, the neovascularization-target ability of decorated iRGD and the improved angiogenesis-inhibition induced by *siVEGF/iRGD*-NPs has been demonstrated (Figure 6): compared to NPs, the iRGD decoration leads to ~2-fold stronger anti-angiogenesis, and ~1.6-fold higher silencing VEGF mRNA. Finally, in a nude-mouse bearing breast cancer model, after intravenous injection, *siVEGF/iRGD*-NPs causes ~1.36-fold higher tumor-growth inhibition and ~1.4-fold down-regulated VEGF protein expression with lower toxicity (more weight gain).

Conclusion

In summary, we have developed a tumor-targeting and penetrating siRNA delivery system of siRNA/iRGD-NPs for anti-tumor therapy by a facile physical method of self-assembly. By successively co-incubating siRNA and then iRGD with lipopolysaccharide-amine nanopolymersomes (NPs), iRGD and siRNA can be successfully loaded by NPs with 100% encapsulation efficiency. The introduction of iRGD onto siRNA-loaded NPs endows the system with the improved tumor/neo-endothelial cells targeting and penetrating bioactivity, the strengthened silencing of target gene, and thus the increased targeted anti-tumor efficacy and decreased toxicity. Because lipopolysaccharide-amine is an amphiphilic, amphoteric, and water-soluble polymer with the ability to self-assemble into nanopolymersomes in water, it can simultaneously load multiple medications including hydrophilic, hydrophobic, amphiphilic, or charged molecules by co-incubation via electrostatic interactions, hydrogen bonds, and hydrophobic interactions. This property makes it easy to construct a compound anti-tumor system composed of Lipopolysaccharide-amine, tumor-targeting/-penetrating ligands, anticancer drugs, nucleic acids, etc. Therefore, this research possibly paves an alternative way for innovative targeted composite anti-tumor medications with high efficiency and low toxicity, and may find wide applications in broad-spectrum anti-tumor treatments in the future.

Acknowledgments

We would like to thank Mr Wenxiao Teng at the history department, College of Arts & Sciences, Syracuse University, USA for his help in English checking of this manuscript. This work was supported by the Guangzhou Science and Technology Plan Project (201803010102) and the Natural Science Foundation of Guangdong Province (2020A1515011207).

Disclosure

The authors declare no conflicts of interest in this work.

References

1. Paunovska K, Loughrey D, Dahlman JE. Drug delivery systems for RNA therapeutics. *Nat Rev Genet.* 2022;23(5):265–280. doi:10.1038/s41576-021-00439-4
2. Mendes BB, Conniot J, Avital A, et al. Nanodelivery of nucleic acids. *Nat Rev Method Primers.* 2022;2(1):24. doi:10.1038/s43586-022-00104-y
3. de Lázaro I, Mooney DJ. Obstacles and opportunities in a forward vision for cancer nanomedicine. *Nat Mater.* 2021;20(11):1469–1479. doi:10.1038/s41563-021-01047-7
4. Seyyednia E, Oroojalian F, Baradaran B, Mojarrad JS, Mokhtarzadeh A, Valizadeh H. Nanoparticles modified with vasculature-homing peptides for targeted cancer therapy and angiogenesis imaging. *J Control Release.* 2021;338:367–393. doi:10.1016/j.jconrel.2021.08.044
5. Chen M, Dong C, Shi S. Nanoparticle-mediated siRNA delivery and multifunctional modification strategies for effective cancer therapy. *Adv Mater Technol.* 2021;6(10):2001236. doi:10.1002/admt.202001236
6. Nguyen PV, Herve-Aubert K, Chourpa I, Allard-Vannier E. Active targeting strategy in nanomedicines using anti-egfr ligands-a promising approach for cancer therapy and diagnosis. *Int. J. Pharmaceut.* 2021;609:121134. doi:10.1016/j.ijpharm.2021.121134
7. Nitheesh Y, Pradhan R, Hejmady S, et al. Surface engineered nanocarriers for the management of breast cancer. *Mat. Sci. Eng. C-Mater.* 2021;130:112441. doi:10.1016/j.msec.2021.112441
8. Lu L, Zhao X, Fu T, et al. An irgd-conjugated prodrug micelle with blood-brain-barrier penetrability for anti-glioma therapy. *Biomaterials.* 2020;230:119666. doi:10.1016/j.biomaterials.2019.119666
9. Davoodi Z, Shafiee F. Internalizing rgd, a great motif for targeted peptide and protein delivery: a review article. *Drug Deliv Transl Res.* 2022;12(10):2261–2274. doi:10.1007/s13346-022-01116-7

10. Guan J, Guo H, Tang T, et al. Irgd-liposomes enhance tumor delivery and therapeutic efficacy of antisense oligonucleotide drugs against primary prostate cancer and bone metastasis. *Adv. Funct. Mater.* **2021**;31(24):2100478. doi:10.1002/adfm.202100478
11. Wang H, Zhou J, Fu Y, et al. Deeply infiltrating irgd-graphene oxide for the intensive treatment of metastatic tumors through ptt-mediated chemosensitization and strengthened integrin targeting-based antimigration. *Adv. Healthc. Mater.* **2021**;10:e2100536. doi:10.1002/adhm.202100536
12. Yin C, Xiao P, Liang M, et al. Effects of iRGD conjugation density on the in vitro and in vivo properties of cylindrical polymer brushes. *Biomater.* **2022**;10:3236–3244. doi:10.1039/d2bm00468b
13. Huang Z, Teng W, Liu L, Wang L, Wang Q, Dong Y. Efficient cytosolic delivery mediated by polymersomes facilely prepared from a degradable, amphiphilic, and amphoteric copolymer. *Nanotechnology.* **2013**;24(26):265104. doi:10.1088/0957-4484/24/26/265104
14. Huang M, Zhang X, Li J, Li Y, Wang Q, Teng W. Comparison of osteogenic differentiation induced by sinoggin and pbmp-2 delivered by lipopolysaccharide-amine nanopolymersomes and underlying molecular mechanisms. *Int J Nanomedicine.* **2019**;14:4229–4245. doi:10.2147/IJN.S203540
15. Wang Q, Chen Y, Wang L, Zhang X, Huang H, Teng W. Stability and toxicity of empty or gene-loaded lipopolysaccharide-amine nanopolymersomes. *Int J Nanomed.* **2015**;10:597–608. doi:10.2147/IJN.S74156
16. Teng W, Huang Z, Chen Y, Wang L, Wang Q, Huang H. Pvegf-loaded lipopolysaccharide-amine nanopolymersomes for therapeutic angiogenesis. *Nanotechnology.* **2014**;25(6):065702. doi:10.1088/0957-4484/25/6/065702
17. Del Duca D, Werbowetski T, Del Maestro RF. Spheroid preparation from hanging drops: characterization of a model of brain tumor invasion. *J Neuro-Oncol.* **2004**;67(3):295–303. doi:10.1023/B:NEON.0000024220.07063.70
18. Huang X, Liu C, Kong N, et al. Synthesis of siRNA nanoparticles to silence plaque-destabilizing gene in atherosclerotic lesional macrophages. *Nat Protoc.* **2022**;17(3):748–780. doi:10.1038/s41596-021-00665-4
19. Zhao Y, Wang W, Guo S, et al. Polymetformin combines carrier and anticancer activities for in vivo siRNA delivery. *Nat Commun.* **2016**;7(1):11822. doi:10.1038/ncomms11822
20. Xu B, Zhang Y, Yang H, et al. Sivegf-loaded nanoparticle uptake by tumor-associated vascular endothelial cells for hepatocellular carcinoma. *Nanomedicine-UK.* **2020**;15(13):1297–1314. doi:10.2217/nnm-2020-0082
21. Guo Z, Li S, Liu Z, Xue W. Tumor-penetrating peptide-functionalized redox-responsive hyperbranched poly (amido amine) delivering siRNA for lung cancer therapy. *ACS Biomater Sci Eng.* **2018**;4(3):988–996. doi:10.1021/acsbomaterials.7b00971
22. Wonder E, Simón-Gracia L, Scodeller P, et al. Competition of charge-mediated and specific binding by peptide-tagged cationic liposome–DNA nanoparticles in vitro and in vivo. *Biomaterials.* **2018**;166:52–63. doi:10.1016/j.biomaterials.2018.02.052
23. Hu C, Yang X, Liu R, et al. Coadministration of irgd with multistage responsive nanoparticles enhanced tumor targeting and penetration abilities for breast cancer therapy. *ACS Appl Mater Inter.* **2018**;10(26):22571–22579. doi:10.1021/acsami.8b04847
24. Patnaik S, Gupta KC. Novel polyethylenimine-derived nanoparticles for in vivo gene delivery. *Expert Opin Drug Del.* **2013**;10(2):215–228. doi:10.1517/17425247.2013.744964
25. Hu B, Zhong L, Weng Y, et al. Therapeutic siRNA: state of the art. *Signal Transduct Target Ther.* **2020**;5(1):101. doi:10.1038/s41392-020-0207-x
26. Zhou Q, Dong C, Fan W, et al. Tumor extravasation and infiltration as barriers of nanomedicine for high efficacy: the current status and transcytosis strategy. *Biomaterials.* **2020**;240:119902. doi:10.1016/j.biomaterials.2020.119902

International Journal of Nanomedicine

Dovepress

Publish your work in this journal

The International Journal of Nanomedicine is an international, peer-reviewed journal focusing on the application of nanotechnology in diagnostics, therapeutics, and drug delivery systems throughout the biomedical field. This journal is indexed on PubMed Central, MedLine, CAS, SciSearch®, Current Contents®/Clinical Medicine, Journal Citation Reports/Science Edition, EMBase, Scopus and the Elsevier Bibliographic databases. The manuscript management system is completely online and includes a very quick and fair peer-review system, which is all easy to use. Visit <http://www.dovepress.com/testimonials.php> to read real quotes from published authors.

Submit your manuscript here: <https://www.dovepress.com/international-journal-of-nanomedicine-journal>